

# Invisible Decay of Muonium: Tests of the Standard Model and Searches for New Physics

S.N. Glinenko<sup>1</sup>, N.V. Krasnikov<sup>1</sup>, and V.A. Matveev<sup>1,2</sup>

<sup>1</sup> Institute for Nuclear Research of the Russian Academy of Sciences, 117312 Moscow, Russia

<sup>2</sup> Joint Institute for Nuclear Research, 141980 Dubna, Russia

(Dated: September 4, 2012)

The invisible decay of muonium atom  $M \rightarrow \text{invisible}$ ,  $M = \mu^+e^-$  bound state, is expected to be a very rare process which has never been experimentally tested. In the standard model it goes via the  $\mu^+e^-$  annihilation into two neutrinos, with the branching fraction predicted to be  $Br(M \rightarrow \nu_\mu\nu_e) = 6.6 \times 10^{-12}$  with respect to the ordinary muon decay rate. Using the reported experimental results on searches for muonium-antimuonium conversion at PSI we set the first limit  $Br(M \rightarrow \text{invisible}) < 4.6 \times 10^{-3}$  (90% C.L.), while still leaving a big gap of about nine orders of magnitude between this bound and the predictions. To improve substantially the limit, we proposed to perform an experiment dedicated to the sensitive search for the  $M \rightarrow \text{invisible}$  decay. A feasibility study of the experimental setup shows that the sensitivity of the search for this decay mode in branching fraction  $Br(M \rightarrow \text{invisible})$  at the level of  $10^{-12}$  could be achieved. If the proposed search results in a substantially higher branching fraction than predicted, say  $Br(M \rightarrow \text{invisible}) \simeq 10^{-10}$ , this would unambiguously indicate the presence of new physics. We point out that such a possibility may occur due the muonium transition into a hidden sector and consider, as an example, muonium-mirror muonium conversion in the mirror matter model. A result in agreement with the Standard Model prediction would provide a theoretically clean check of the pure leptonic bound state annihilation through the charged current weak interactions, and provide constraints for further attempts beyond the Standard Model. We believe our work provides strong motivations to perform the proposed experiment on search for the invisible decay of muonium in near future.

PACS numbers: 14.80.-j, 12.20.Fv, 13.20.Cz

## I. INTRODUCTION

Experimental studies of particles invisible decays, i.e. transitions to an experimentally unobservable final state, played an important role both in development of the Standard Model (SM) and in constraining its extensions [1]. It is worth to remember the determination of the number of lepton families in the SM through the precision measurements of the  $Z \rightarrow \text{invisible}$  decay rate. In recent years, searches for invisible particle decays have received considerable attention. One could mention experiments looking for extra dimensions with invisible decay of positronium ( $\text{Ps} = e^+e^-$  bound state) [2, 3], baryonic number violation with nucleon disappearance at SNO [4], BOREXINO [5], and KamLAND [6], see also [7], electric charge nonconserving electron decays  $e^- \rightarrow \text{invisible}$  [8], neutron-mirror neutron oscillations at PSI [9] and the ILL reactor [10], neutron disappearance into another brane world [11], and motivated by various models of physics beyond the SM searches for invisible decays of  $\pi^0$  mesons at E949 [12],  $\eta$  and  $\eta'$  mesons at BES [13], heavy  $B$  meson decays at Belle [14], BaBar [15], BES [16] and invisible decays of the Upsilon(1S) resonance at CLEO [17]. There are also proposals for new experiments to search for electric charge nonconservation in the muon decay  $\mu^+ \rightarrow \text{invisible}$  [18], and mirror type dark matter through the invisible decays of orthopositronium in vacuum [19].

Muonium ( $M$ ), the  $\mu^+e^-$ -bound state, is a particularly interesting system for high precision tests of the

SM and searches for new physics. Many interesting experiments performed or planned with muonium were motivated by tests of bound state quantum electrodynamics (QED) in measurements of the muonium hyperfine splitting [20] and 1s-2s interval [21], searches for the lepton number violation in muonium to anti-muonium conversion [22], tests of fundamental symmetries, such as CPT [23], probe of antimatter gravity in the free gravitational fall of muonium [24], and other areas of research [25–27].

As far as the muonium invisible decay is concerned, this process has never been experimentally tested. However, there are several interesting motivations for such experiment to be performed. First, the decay is predicted to exist in the SM at the experimentally achievable today level. Hence, its observation for the first time would be an interesting test of the SM. Second, the decay may occur in some low-mass dark matter scenarios, most of which require coupling between the SM and hidden sectors. For instance, we show that in the mirror matter model such coupling could significantly enhance the  $M \rightarrow \text{invisible}$  decay rate, thus making it very attractive for direct high sensitivity searches. If the  $M \rightarrow \text{invisible}$  decay is observed at a rate higher than the SM prediction, it would be a strong evidence for the existence of new physics beyond the SM.

In this paper we obtain the first limit on the decay  $M \rightarrow \text{invisible}$  and show that it could be significantly improved in a new proposed high-statistics and low-background experiment. We also show that the expected level of the experimental sensitivity allows for the observation of this decay mode for the first time at a rate

predicted by the SM. The rest of the paper is organized as follows. In Sec. II we briefly review the standard model decay rate of muonium and phenomenology of the muonium to anti-muonium conversion. In Sec. III the exact mirror model, the effect of oscillation of ordinary muonium to the mirror one, and its experimental consequences are discussed. The first limit of the branching fraction for the decay  $M \rightarrow invisible$  is obtained from available experimental data in Sec. IV. The experimental technique and the preliminary design of the experiment, detector components, simulations of the signal and background sources, as well as the expected sensitivity are discussed in detail in Sec. V. Sec. VI contains concluding remarks.

## II. MUONIUM DECAY IN THE STANDARD MODEL AND PHENOMENOLOGY OF $M \rightarrow \bar{M}$ CONVERSION

The muonium atom consists of a positive muon and an electron, which are leptons from two different generations. To our current knowledge these are particles without any known internal structure. This makes muonium an ideal system for testing QED and fundamental symmetries in physics [28], and allows to calculate muonium properties to very high accuracy within the framework of the bound state QED. For example, for the hyperfine structure the theoretical predictions and measurements agree substantially better than for hydrogen atoms [29].

As discussed previously, muonium atom, similar to the lightest known exotic hydrogen-like atom positronium, is bounded by the electromagnetic (e-m) interaction. However, differently from positronium the muonium cannot self-annihilate through the e-m interaction because it would violate the lepton number conservation. Instead, the SM allows the self-annihilation of muonium into neutrino pair through the lepton number conserving weak interaction. At the current level of experimental and theoretical precision this are the only interactions present in the muonium system.

In the SM muonium is unstable mainly due to the decay of muon  $\mu^+ \rightarrow e^+ \nu_e \bar{\nu}_\mu$ . Its decay rate in vacuum coincides with those of the muon decay given by

$$\Gamma(M \rightarrow e^+ \nu_e \bar{\nu}_\mu e^-) = \Gamma(\mu^+ \rightarrow e^+ \nu_e \bar{\nu}_\mu) = \frac{G_F^2 m_\mu^5}{192\pi^3}. \quad (1)$$

Here  $G_F = 10^{-5} m_p^{-2}$  is the Fermi constant and  $m_p$ ,  $m_\mu$  are the proton and muon masses, respectively. In matter, muonium is typically formed in the singlet or triplet state, with the total angular momentum equal 0 or 1, respectively. The SM predicts direct annihilation of the triplet muonium,  $J^{PC} = 1^{--}$  bound state, into neutrino antineutrino pair  $M \rightarrow \nu_e \bar{\nu}_\mu$  with a very small decay rate. The corresponding branching fraction  $Br(M \rightarrow$

*invisible*) is calculated to be [30]

$$\begin{aligned} Br(M \rightarrow invisible) &= \frac{\Gamma(M \rightarrow \nu_e \bar{\nu}_\mu)}{\Gamma(\mu \rightarrow e^+ \nu_e \bar{\nu}_\mu)} = \\ &= 48\pi\alpha^3 \left(\frac{m_e}{m_\mu}\right)^3 \approx 6.6 \times 10^{-12}, \end{aligned} \quad (2)$$

where  $\alpha$  is the fine-structure constant, and  $m_e$  is the electron mass. The singlet muonium cannot decay into two neutrinos, as it contradicts to momentum and angular momentum conservation simultaneously.

Very interesting feature of muonium is the possibility of conversion(or oscillation) into its antiatom, i.e. the  $\mu^- e^+$  bound state [31–33]. This reaction violates the conservation of lepton flavor numbers by two units ( $\Delta L_{e,\mu} = \pm 2$ ) that makes searches for the  $M - \bar{M}$  conversion especially interesting due to experimental observations of lepton flavor violation in neutrino oscillations.

The existence of muonium to anti-muonium conversion is predicted in different extensions of the SM. The simplest way to understand the phenomenology of  $M - \bar{M}$  conversion is the use of the effective four fermion interaction of the  $(V - A)(V - A)$  type [32], namely

$$L_{M\bar{M}} = \left(\frac{G_{M\bar{M}}}{\sqrt{2}}\right) \bar{\mu} \gamma_\lambda (1 - \gamma_5) e \bar{\mu} \gamma^\lambda (1 - \gamma_5) e + H.c., \quad (3)$$

where  $G_{M\bar{M}}$  is a coupling constant characterizing the strength of a new flavor violating interaction. In the absence of an external magnetic field the muonium and anti-muonium have the same ground-state energy levels. Flavor violating interaction (3) would cause a splitting of their energy levels by amount [32, 33]

$$\delta \equiv 2 < \bar{M} | L_{M\bar{M}} | M > = \frac{8G_F}{\sqrt{2}n^2\pi a_0^3} \left(\frac{G_{M\bar{M}}}{G_F}\right). \quad (4)$$

Here  $n$  is the principal quantum number of the muonium atom and  $a_0 = \frac{m_e + m_\mu}{m_e m_\mu \alpha}$  is the Bohr radius of the muonium. Numerically, for the ground state of muonium ( $n = 1$ )

$$\delta = 1.5 \times 10^{-12} \left(\frac{G_{M\bar{M}}}{G_F}\right) (eV). \quad (5)$$

The  $M - \bar{M}$  conversion is analogous to the  $K^0 - \bar{K}^0$  mixing. If a muonium atom is formed at  $t = 0$  in vacuum, it could oscillate into an anti-muonium atom. For a small  $t$  value the probability of the oscillation is represented in the form [32]

$$P_{M\bar{M}}(t) = \sin^2\left(\frac{\delta t}{2}\right) \cdot \Gamma_\mu e^{-\Gamma_\mu t} \approx \left(\frac{\delta t}{2}\right)^2 \cdot \Gamma_\mu e^{-\Gamma_\mu t}. \quad (6)$$

Here  $\Gamma_\mu \equiv \Gamma(\mu^+ \rightarrow e^+ \nu_e \bar{\nu}_\mu)$  is the muon decay width. The total conversion probability after integration over time is equal to

$$\begin{aligned} P_{M\bar{M}} &= \int_0^\infty \rho_{M\bar{M}}(t) dt = \frac{|\delta|^2}{2(|\delta|^2 + \Gamma_\mu^2)} \\ &= 2.56 \times 10^{-5} \cdot \left(\frac{G_{M\bar{M}}}{G_F}\right)^2. \end{aligned} \quad (7)$$

The best current experimental limit on the  $M \rightarrow M'$  conversion leads to bound  $|G_{M\bar{M}}| \leq 0.003 \cdot G_F$  [22]. It should be noted that in the presence of collisions with residual gas molecules or Zeeman splitting due to nonzero external magnetic field, the  $M - \bar{M}$  transitions become highly suppressed.

### III. MUONIUM CONVERSION IN MIRROR MATTER MODEL

The idea that along with the ordinary matter may exist its exact mirror copy is an old one [34, 35]. This new hidden gauge sector is predicted to exist if parity is unbroken symmetry of nature, for an excellent review see Ref. [36]. In accordance with this idea each ordinary particle of the SM has a corresponding mirror partner of exactly the same mass as the ordinary one, so that the properties of the mirror particles completely mirror those of the ordinary particles. The parity symmetry interchanges the ordinary particles with the mirror ones. For example, the mirror proton and mirror electron are stable and interact with the mirror photon in the same way in which the ordinary proton and electron interacts with the ordinary photons. The mirror particles couple very weakly to the ordinary particles, hence they are not produced abundantly in our experiments. In the modern language of gauge theories, the mirror particles are all singlets under the standard  $G = SU(3) \otimes SU(2)_L \otimes U(1)_Y$  gauge interactions [37–39]. Instead the mirror particles interact with a set of mirror gauge particles, so that the gauge symmetry of the theory is doubled, i.e. the ordinary particles are singlets under the mirror gauge symmetry. Parity is conserved because the mirror particles experience  $V+A$ , i.e. right-handed mirror weak interactions while the ordinary particles experience the usual  $V-A$ , i.e. left-handed weak interactions. Mirror matter, which interacts with ordinary matter presumably via gravity and possibly by other very weak forces, is dark in terms of the SM interactions, and could be a viable candidate for dark matter, see e.g. Refs.[39–43]. For instance, it is argued that annual modulations of the signal observed by the DAMA Collaboration are caused by the mirror dark matter scattering in their detector [44–47].

The gauge group of our world and mirror world is assumed to be [37]

$$G_{tot} = G_{SM} \otimes G_M, \quad (8)$$

where the SM gauge group  $G_{SM}$  coincides with the mirror world gauge group  $G_M$ . The interaction between our and mirror sectors could be transmitted by some gauge singlet particles interacting with both sectors. Such kind of interaction could explain the baryon asymmetry of the Universe [48], some fraction of dark matter in the Universe [43], and can also induce the particle mixing and oscillation phenomena between the ordinary and mirror sectors. Any neutral, elementary or composite particle, can have a mixing with its mirror duplicate, such

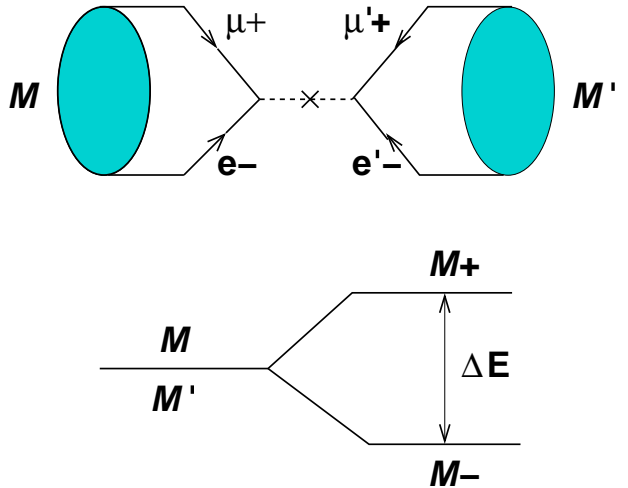


FIG. 1: The double degeneracy between mass eigenstates of ordinary ( $M$ ) and mirror ( $M'$ ) muonium is broken when a small mixing is included.

as photon-mirror photon [49, 50], neutrino-mirror neutrino [37, 38], etc. which results in testable experimental effects. For example, the neutron-mirror neutron mixing via a small mass term  $\epsilon(nn' + n'n)$  proposed in [48], results in ordinary neutron anomalous disappearance, in addition to their decays or absorption due to SM interactions. At present, there are performed and proposed searches for mirror matter via the invisible decay of orthopositronium in vacuum [19, 49–55], through neutron-mirror neutron oscillations [48, 56, 57], and via Higgs-mirror Higgs mixing at LHC [58–60].

As mentioned previously, in mirror world model there must exist the mirror muonium which is the bound state of a mirror muon  $\mu'$  and a mirror positron  $e'^+$  with the same mass and decay width as the ordinary muonium. We could assume the existence of a (super)weak interaction invariant under the gauge group  $G_{tot}$ , which allows transitions between the ordinary and mirror muonium. Such effective interaction can be written in a form analogous to (3)

$$L_{MM'} = \left( \frac{G_{MM'}}{\sqrt{2}} \right) \bar{\mu} \gamma_\lambda (1 + \gamma_5) e \bar{e}' \gamma_\lambda (1 - \gamma_5) \mu' + H.c. \quad (9)$$

where  $G_{MM'}$  is a coupling constant characterizing the strength of the  $M - M'$  transition, and  $e'$  and  $\mu'$  are the mirror electron and muon fields, correspondingly. The interaction (9) leads to conversion of ordinary muonium to mirror muonium, as schematically illustrated in Fig. 1. The interaction (9) breaks the degeneracy between  $M$  and  $M'$  states, so that the vacuum energy eigenstates are  $M^+ = (M + M')/\sqrt{2}$  and  $M^- = (M - M')/\sqrt{2}$ , which are split in energy by  $\Delta E$  given by an expression similar to (4), see Fig.1. The interaction eigenstates are maximal combinations of mass eigenstates which implies that  $M$  oscillates into  $M'$ . Thus, a system which is pure muonium at  $t = 0$  will develop an admixture of mirror

muonium at a later time. In closed analogy with the case of muonium anti-muonium conversion one can find that the probability of seeing the system in vacuum decay as mirror muonium  $M' \rightarrow e^+ \nu'_e \nu'_\mu + e^-$  rather than as ordinary muonium  $M \rightarrow e^+ \nu_e \nu_\mu + e^-$  is given by

$$P(M') = \frac{1}{2} \frac{\delta^2}{\delta^2 + \Delta^2 + \lambda^2} \quad (10)$$

where  $\lambda = 0.45 \times 10^6 \text{ sec}^{-1}$ , or  $3 \times 10^{-10} \text{ eV}$ , and  $\Delta$  is any additional splitting of  $M$  and  $M'$ , by external electromagnetic fields. A detail discussions of the effects of collisions and external fields on oscillation probability of a similar system, positronium, can be found in Ref.[61]. Estimating  $\delta$  by using (9) results in the integral probability of muonium to mirror muonium conversion determined by (for  $\Delta = 0$ )

$$P_{MM'} = 2.56 \times 10^{-5} \cdot \left( \frac{G_{MM'}}{G_F} \right)^2. \quad (11)$$

Because mirror muonium decays into a mirror electron, positron and neutrinos the experimental signature of the  $M - M'$  conversion is the invisible decay  $M \rightarrow \text{invisible}$  of the ordinary muonium in vacuum. Current bounds on coupling constant  $G_{MM'}$  are rather weak. For  $G_{MM'} = G_F$  the branching fraction of the ordinary muonium decay into invisible mirror state is  $Br(M \rightarrow \text{invisible}) = 2.56 \times 10^{-5}$ , which is seven orders of magnitude higher than the predicted by the SM branching fraction of Eq.(2). Thus, we see that in the mirror model it is possible to have nonzero conversion of our muonium to mirror muonium. The signature of such conversion is the decay  $M \rightarrow \text{invisible}$  and, moreover, it is possible to expect some enhancement of this decay rate. Similar to the  $M - \bar{M}$  conversion, the probability  $P_{MM'}$  can be affected by an additional splitting of  $M$  and  $M'$  states due to an external electric or magnetic field [32, 61]. It might also be suppress, if there is a high collision rate of muonium atoms with the cavity walls or residual gas molecules in the experiment.

Note that some extensions of the SM allow the  $M \rightarrow \text{invisible}$  decay. For instance, in model with additional sterile neutrino, interaction

$$L = G' \bar{\mu} \gamma_\nu (1 - \gamma_5) e \bar{\nu}_s \gamma^\nu (1 - \gamma_5) \nu_s + h.c.$$

results in invisible muonium decays into sterile neutrino  $M \rightarrow \nu_s \bar{\nu}_s$ . However, constraints obtained from the agreement between the measured and predicted properties of the  $\mu$ -decay [1] lead to a strong bound  $\Gamma(M \rightarrow \bar{\nu}_s \nu_s) \leq O(10^{-2}) \Gamma(M \rightarrow \nu_e \bar{\nu}_\mu)$  on sterile neutrino decay width, which makes it not very exciting for further considerations.

#### IV. EXPERIMENTAL LIMIT ON THE $M \rightarrow \text{invisible}$ DECAY

Consider now bound on the invisible decay of the  $M$  state, which can be obtained from existing experimental

data. If an exotic  $M \rightarrow \text{invisible}$  decay exists, it would contribute to the total muonium decay rate:

$$\tau_M^{-1} = \Gamma_M(M \rightarrow \text{all}) = \Gamma_\mu + \Gamma(M \rightarrow \text{invisible}) + \dots \quad (12)$$

and, hence decrease the determined muonium lifetime  $\tau_M$  in vacuum. To estimate the allowed contribution of  $\Gamma(M \rightarrow \text{invisible})$  to Eq.(12), one could compare the measured muonium decay rate in vacuum to a predicted muon decay rate, obtained in measurements which are not affected by the muonium disappearance effect discussed above. To avoid confusion with the decay  $\mu^+ \rightarrow \text{invisible}$ , here we assume that both  $\mu^+$  and  $e^-$  disappear in the detector.

In order to obtain limit on the branching fraction

$$Br(M \rightarrow \text{invisible}) = \Gamma(M \rightarrow \text{invisible}) / \Gamma(\mu \rightarrow e \nu) \quad (13)$$

we use the results of the most precise experiment on  $M - \bar{M}$  conversion performed at PSI [22]. In this experiment muonium was formed in a layer of  $\text{SiO}_2$  powder and escaped into the vacuum after diffusion to the layer surface with a diffusion length  $L = \sqrt{D_M \tau_\mu}$ , where  $D_M$  and  $\tau_M$  are the muonium diffusion constant and lifetime, respectively [62]. The distribution of time intervals between the stop of a muon and the detected signal from the muonium decay in vacuum is shown in Fig. 5. The number  $N_M^{\text{vac}}(t)$  of  $M$  decays observed as a function of time and can be well approximated by [62]

$$N_M^{\text{vac}}(t) = f \exp(-t/\tau_M) \sqrt{D_M t} \quad (14)$$

where  $f$  is a normalization constant. The fit of the experimental distribution shown in Fig. 5 to the function (14) results in

$$\tau_M^{\text{exp}} = 2.247 \pm 0.047 \mu\text{s}. \quad (15)$$

The value of the positive muon mean lifetime  $\tau_\mu$  is taken from results of its measurements by the MuLan collaboration has reported to a precision of 11 ppm [63]. Using the new world average [1]

$$\tau_\mu = 2.197019(21) \mu\text{s} \quad (16)$$

and comparing Eq.(15) and Eq.(16), one finds

$$Br(M \rightarrow \text{invisible}) = \frac{\Gamma(M \rightarrow \text{invisible})}{\Gamma(\mu^+ \rightarrow \text{all})} < 4.6 \times 10^{-3} \text{ (90\%C.L.)}. \quad (17)$$

There is still nine orders of magnitudes difference between the limit of Eq.(17) and the SM prediction (2). In the next Section we show how this limit can be significantly improved in the new proposed experiment.

#### V. DIRECT EXPERIMENTAL SEARCH FOR THE $M \rightarrow \text{invisible}$ DECAY

The decays  $M \rightarrow \text{invisible}$  are rare events and their observation presents a challenge for the detector design

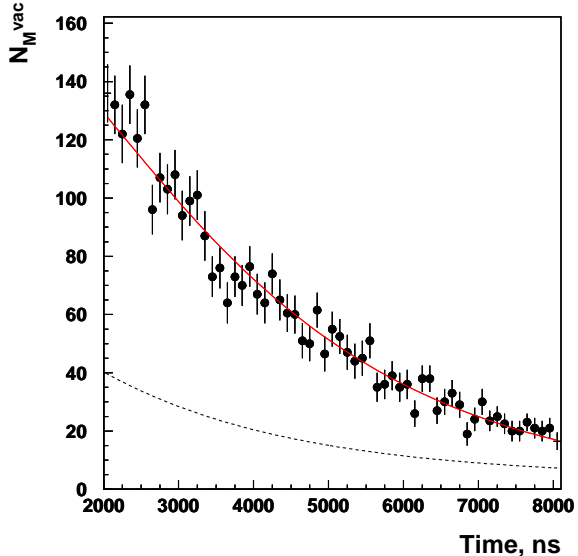


FIG. 2: The distribution of time intervals  $t$  between the stop of a muon in the  $\text{SiO}_2$  target and signal from the decay of muonium escaping into vacuum for  $t > 2000$  ns in the PSI experiment on search for  $M - \bar{M}$  conversion [22]. Experimental points and dashed curve representing an exponential background are from Ref.[22], the solid line is our fit to the data.

and performance. Here, we focus mainly on discussions of the experimental setup to search for the decay  $M \rightarrow \text{invisible}$  in vacuum, which is also sensitive to the muonium - mirror muonium conversion. The similar setup without vacuum requirements is simpler, it would provide better sensitivity and can be used for the first observation of the decay  $M \rightarrow \text{invisible}$  and search for new exotic channels of this decay mode which are not affected by the presence of matter of external fields.

The main components of the experimental setup to search for the invisible decay of muonium are schematically illustrated in Fig. 3, see also [18]. The setup is equipped with a high efficiency muon tagging system, high hermeticity electromagnetic calorimeter (ECAL), and an intelligent trigger system. The experiment employs a surface  $\mu^+$  beam, which is produced in a target and transported to the detector in an evacuated beam line tuned to  $\sim 26$  MeV/c. Such the world's brightest continuous surface muon beam with intensity  $\simeq 10^7 \mu/s$  is available at the Paul Scherrer Institut (PSI) [64]. This beam was used, for example for a sensitive search for  $M - \bar{M}$  conversion [22]. Positively charged muons pass through a  $\sim 100 \mu\text{m}$  thick beam counters ( $S_{1,2}$ ) and focused into a vacuum cavity through a narrow aperture closed by the beam counter  $S_3$  and after passing through the counter  $S_4$  strike the  $\text{SiO}_2$  aerogel (or  $\text{SiO}_2$  powder) target ( $T$ ) used for the muonium atom formation [65, 66]. The energy of entering muons is degraded by the counters material to maximize the muon stopping

rate. Muonium atoms are formed by the electron capture with efficiency  $\simeq 60\%$  per  $\mu^+$  stopped in the target. Most of the atoms emerge from the target grains into the intergranular voids. With a mean-free path of  $\simeq 1$  cm, muonium is able to diffuse through the network of voids over distances longer than the target thickness and escape through the surface into vacuum [28]. Muonium undergoes of the order  $10^5 - 10^7$  collisions with the silica grain walls, those number depends on the depth of muonium formation, and approach thermal equilibrium. Then, on average, 3.3% of them leave the target surface with thermal Maxwell-Boltzmann velocity distribution at the temperature of the target [65]. The fact that muonium confined to the voids is expected to be almost fully thermalized, was confirmed by a separate experiment on  $M$ 's emitted into vacuum from a mesaporous silica film at cryogenic temperatures [67]. Although the  $M$  kinetic energy distribution is nominally that of Maxwell-Boltzman emission, one might expect a higher-energy tail of  $M$ 's formed from backscattered muons that never approached thermalization. These  $M$  events are distinct from the thermal  $M$ 's that has diffused out of the target, however their intensity is expected to be very small. The fraction of muonium atoms produced in the target that decay either in the target or in vacuum can be determined relative to the number of muons on the target with a technique described in Ref.[22].

The target is surrounded by a hermetic  $4\pi$  electromagnetic calorimeter (ECAL) to detect energy deposition from the decay  $M \rightarrow \text{all}$  of muoniums produced in  $T$ . As shown in Fig. 3, before muons reach the entrance to the vacuum cavity, they bend in a magnetic field. The purpose of employing the magnet is twofold: (i) to provide a transverse kick to positive muons in order to allow them to enter the vacuum cavity through the narrow aperture, and (ii) to detect photons, positrons, or muons that could escape cavity through the entrance aperture by a set of ECAL counters placed around the muon bend region. This additional detector is placed upstream of the entrance aperture, as shown in Fig. 3.

The energy deposition readout in the ECAL is triggered by a tag signal of the muon appearance on the target, which is defined as the coincidence of the four signals from a muon passing the beam counters  $S_{1-4}$ . To enhance significance of the muon tag the time-of-flight information can be used. For the muon beam momentum of 26 MeV/c, the latter corresponds to about 1.3 ns per 10 cm of the muon path length.

For the ordinary muonium decay (1) the experimental signature is the ECAL energy deposition from a single decay positron with energy  $E_{e^+} = m_\mu - E_{\nu_e} - E_{\nu_\mu}$ , where  $E_{\nu_e}, E_{\nu_\mu}$  are the electron and muon neutrino energy, respectively. The experimental signature of the  $M \rightarrow \text{invisible}$  decay is the apparent disappearance of the energy deposition  $E = m_\mu + m_e$  in the ECAL. In other words, the signature of the  $M \rightarrow \text{invisible}$  decays is an event with the sum of the ECAL crystal energies deposited by the final-state particles equal zero. Zero en-

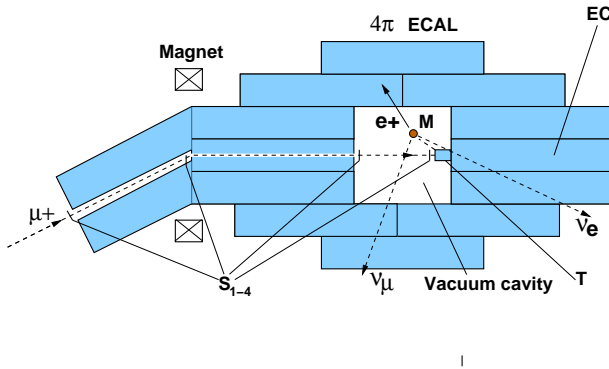


FIG. 3: Schematic illustration of the experimental setup to search for the muonium invisible decay. The beam of surface  $\mu^+$ 's passing through the beam defining counters  $S_{1-4}$  is focused into a vacuum cavity through a narrow aperture and strike the  $\text{SiO}_2$  aerogel target ( $T$ ) used for the muonium atom formation. Shown are also the  $4\pi$  hermetic BGO electromagnetic calorimeter (ECAL), the ECAL endcap counter EC used as a light guide for the light produced in the beam counter  $S_4$ , and the magnet used to deflect the beam. The counters  $S_{1-3}$  and the upstream ECAL counters are also used as a veto against photons, decay positrons or backscattered muons that could escape the cavity through the entrance aperture.

ergy is defined in this case as an energy deposition below of a certain ECAL energy threshold,  $E_{tot} < E_{th}$ . The expected distribution of energy deposited in the ECAL from  $\mu^+$ 's stopped in the target is shown in Fig. 4. The distribution is a sum of two spectra from  $\mu^+ \rightarrow \text{all}$  and  $M \rightarrow \text{all}$  decays and is discussed in detail below in Sec.A.

To estimate the sensitivity of the proposed experiment a feasibility study based on GEANT4 [68] Monte Carlo simulations have been performed. The beam of positive muons is stopped in the central part of the cylindrical target of  $\text{SiO}_2$  aerogel with the density about  $35 \text{ mg/cm}^3$  and of thickness  $8 \text{ mg/cm}^2$  and supported in vacuum by an aluminum foil with an inclination with respect to the muon beam axis. Similar target was previously used as a convertor of muon to muonium atoms in the experiment of Ref.[22]. The ECAL is an array of  $\simeq 100$  BGO counters each of  $52 \text{ mm}$  in diameter and  $220 \text{ mm}$  long, which was previously used in the PSI experiment on precise measurements of the  $\pi \rightarrow e + \nu$  decay rate [69]. Timing and energy deposition information from each BGO crystal can be digitized for each event. The processing of the BGO counter signals is described in detail in Ref.[69], see also [3, 70].

### A. Background for the $M \rightarrow \text{invisible}$ decay

The background processes for the  $M \rightarrow \text{invisible}$  decay can be classified as being due to beam-related, physical, and detector-related backgrounds. To investigate these backgrounds down to the level  $Br(\mu \rightarrow \text{invisible}) \lesssim 10^{-12}$  with the full detector simulation

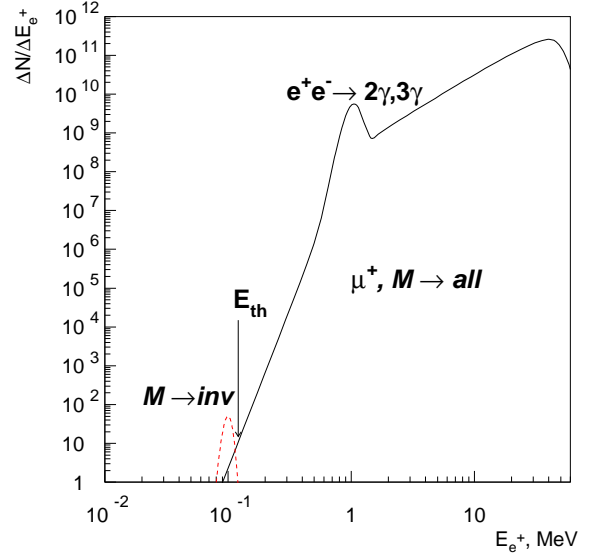


FIG. 4: The expected distribution of energy deposition in the ECAL from  $8 \times 10^{12}$  muons stopped in the target, corresponding to the decays  $\mu^+ \rightarrow \text{all}$  and  $M \rightarrow \text{all}$ . The peak around 1 MeV corresponds to energy deposition from the  $e^+e^- \rightarrow 2\gamma, 3\gamma$  annihilation of decay positrons stopped in the vacuum cavity. The arrow shows the energy threshold for the decay  $M \rightarrow \text{invisible}$  detection. The dashed curve represents the signal from the decay  $M \rightarrow \text{invisible}$  if it exist at the level predicted by the SM.

would require the generation of a very large number of muon decays resulting in a prohibitively large amount of computer time. Consequently, only the most dangerous background processes are considered and estimated with a smaller statistics combined with numerical calculations.

The beam-related backgrounds produce the fake muon tag and can be categorized as being due to a beam particle misidentified as a muon, or several beam particles which produce fake muon tag due to accidental coincidence of signals from  $S_{1-4}$ . The first type of background occurs, e.g. due to the production of slow protons in the target, which enter the detector and produce zero decay energy. Incoming neutrons could scatter in the  $S_{1-4}$  and being accidentally misidentified as  $\mu^+$  could also contribute to the beam background. Identification of the incoming particle as a muon based on the requirements of the delayed by the muon time-of-flight coincidence between the beam counter signals suppressed the single-beam background down to the level  $< 10^{-13}$ . This estimate is obtained under assumption of having Gaussian shape with the time resolution of  $\simeq 1 \text{ ns}$  for the distributions of time-of-flight between counters  $S_{1-4}$ . It is also assumed that the admixture of the other charged particles in the beam is below 1%, which although depends on a particular experimental environment.

For the design shown in Fig.3, the required efficiency

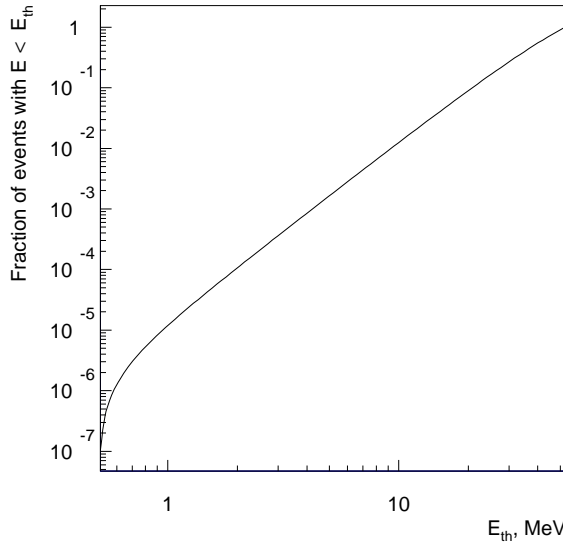


FIG. 5: The fraction of events from the decay  $M \rightarrow e^+ \nu_\mu \nu_e + e^-$  with the positron energy  $E < E_{th}$  as a function of  $E_{th}$ .

for the  $M$  decay energy detection can be obtained only by keeping the amount of passive material in the region of vacuum cavity as small as possible. For example, to remove dead materials from the vacuum cavity walls the cavity could be made directly in a big single crystal or out of a few ECAL central crystals. The light signals produced in the  $S_4$  scintillator counter could be readout through the  $\text{SiO}_2$  transparent target and the ECAL end-cap crystal ( $EC$ ) which acts as a light guide, see Fig. 3. The  $S_4$  signals could be distinguished from the  $EC$  signals due to their significantly different decay times by using the technique described in detail in Ref.[3]. In the presented simulations we did not consider too complicated design of the setup and try to keep it as realistic as possible. The reported further analysis takes into account active materials of the ECAL, passive materials from the target, vacuum cavity walls, and from the ECAL crystals and the target wrapping. The following main sources of physical- and detector-related backgrounds are identified and evaluated:

- the principal muon decay  $\mu \rightarrow e\nu\bar{\nu}$  into the final state with the positron kinetic energy  $E_{kin}$  less than the detection energy threshold  $E_{th}$  ( $\simeq 100$  keV). Indeed, if  $E_{kin} < E_{th}$  the event becomes invisible. To suppress this background, one has to use as low as possible threshold  $E_{th}$  and to performed the experiment with a well separated positive muon beam with an extremely small contamination of negative pions or muons which could mimic the true signal. However, even if the positive muon decays into a low energy positron that stop in the cavity, the later would annihilate into two (or three) photons at a lifetime scale of the order of a few ns.

Thus, for such events the minimum energy deposition in the ECAL will be  $m_{e+} + m_{e-} \simeq 1$  MeV, i.e. well above the threshold, making these events visible, see Fig. 4.

Another way to lose the decay energy is due to the annihilation gammas photo-absorption and/or Compton scattering in the target. In this case, when almost all annihilation energy is deposited in  $T$  the event becomes invisible, which results in a fake  $M \rightarrow invisible$  signal. To suppress this background the target should be optimized in size and made of a low-Z material to minimize cross-section of the photo-absorption which is  $\sigma_{pha} \sim Z^5$ . For example, for a target made of plastic scintillator the probability of both 511 keV photons energy absorption in a volume of  $\simeq 1 \text{ cm}^3$  is found to be less than  $10^{-8}$  [18]. In the  $\text{SiO}_2$  target with the density 35 mg/cm<sup>3</sup> the effect is smaller. The ECAL efficiency with respect to detection of energy from the positron annihilation was checked in the experiment [3] on search for the  $Ps \rightarrow invisible$  decay. For events corresponding to  $2,3\gamma$  annihilation of  $e^+e^-$  pairs at rest with the ECAL energy deposition  $\sim 1$  MeV, the upper limit on the branching fraction of the reaction  $e^+e^- \rightarrow invisible$  was found to be  $Br(e^+e^- \rightarrow invisible) \lesssim 10^{-8}$  at 90% C.L. for the ECAL energy threshold of 80 keV.

The absorption of annihilation photons in the cavity materials has been studied in the proposal on search for the  $oPs \rightarrow invisible$  decay in vacuum of Ref. [19]. Simulations show that the main contribution to the  $\gamma$  inefficiency comes from the total (due to photo-absorption) or fractional (due to Compton effect) photon energy loss in the material of the vacuum cavity. To suppress this background the cavity should be made of a low-Z material to minimize cross-section of the photo-absorption. Distributions of the energy deposited in the dead material surrounding the target region from annihilation events in the target were obtained with simulations for a 0.84 mm thick aluminum pipe and a composition pipe made of 0.04 mm aluminum and 0.800 mm carbon. For the later case the fraction of simulated  $2\gamma$  events with the energy absorbed in the cavity walls  $> 900$  keV, i.e. energy deposited in the ECAL is  $E < 100$  keV, was found to be  $< 10^{-8}$ .

In Fig. 5, the partial muon decay rate  $\Delta\Gamma_\mu$  into a positron with  $E_{e^+} < E_{th}$  is shown as a function of  $E_{th}$ . Taking into account that energy of positrons that stop in the cavity is typically  $E_{kin} < 2 - 3$  MeV, the fraction of such  $e^+$ 's is estimated to be  $P_T \lesssim 10^{-4}$ . Combined probability to get energy deposition in the ECAL from positron annihilation in the cavity  $< 100$  keV is estimated to be  $P_{2\gamma} \lesssim 2 \times 10^{-8}$ . Therefore, this background from inefficient detection of low energy positrons allows potentially to reach sensitivity in the branching ratio of the

invisible muonium decay as small as  $P_T \cdot P_{2\gamma} \simeq 2 \times 10^{-12}$ , assuming the detection energy threshold is as low as  $E_{th} \simeq 100$  keV.

- the loss of the muon decay energy in rare processes of energetic positrons  $e^+ + A \rightarrow \text{invisible}$  with an invisible final state could be induced either by electromagnetic or weak interactions of the positron. For example,  $e^+$  could lose almost all its energy due to emission of a hard photon in the bremsstrahlung process in the target or in the ECAL. The photon could either penetrate the calorimeter without interactions, or could be photo-absorbed by an atomic nucleus resulting in the invisible final state consisted of secondary neutrons. However, due to the charge conservation, there is always a low energy positron in the final state, which produce  $\simeq 1$  MeV energy through the  $e^+e^-$  annihilation of the positron at rest, thus making the event visible. Combined analysis results in this background level  $\lesssim 10^{-13}$ . The background from an energetic positron conversion into proton through the reaction  $e^+ + n \rightarrow p + \bar{\nu}_e$  induced by the charge current weak interaction is found to be negligible.
- Another possible background could be due to the excitation of a long-lived nuclear state via the radiationless annihilation of an energetic positron with a K-shell electron. This is a 3-body reaction  $e^+ + e^- + A \rightarrow A^*$ , where the  $e^+e^-$  annihilation energy is absorbed by the nucleus  $A$ . The cross section for such reaction has not yet been studied in details for the wide class of nuclear isotopes and full range of positron energies. By using the available upper limit on the resonant cross section  $\sigma_{e^+} < 4.3 \times 10^{-26}$  cm $^2$  at 99% C.L. obtained for isotope  $^{115}\text{In}$  with a mono-energetic positron beam of about 90 keV kinetic energy [71] we estimate this background to be  $\lesssim 10^{-13}$ , assuming the  $^{115}\text{In}$  contamination in the cavity and target materials to be at the level below 1 ppm. More detailed study of this background source is required. Note, that in principle, it is possible to excite a nucleus long-lived state with a lifetime  $\tau \gtrsim 60\mu\text{s}$ . However, such excitation levels are present in specific isotopes, such as  $^{115}\text{In}$ , those admixture is expected to be small.
- incomplete ECAL hermiticity: our study identified possible background to the signal as due to energetic decay positrons escaping the detection region though the cavity entrance aperture. This effect increase the disappearance rate of muonium and therefore must be addressed. Consider, e.g. the case when a muon decays either in flight or in the target into a fast positron with momentum pointing exactly to the entrance aperture. Then, the decay positron could be undetected in beam counters  $S_3$  and  $S_2$  due to their inefficiency. The same effect could occur if the incoming muon backscatters either in  $S_4$  or in the target without losing too much

energy, and escapes the detection in counters  $S_{2,3}$ . However, due to presence of the magnetic field in the vicinity of the entrance to the cavity the trajectory of the escaping positron or muon is bended up and it would be detected by the ECAL counters.

The probability for a particle to escape detection in this case can be estimated as

$$P_{esc} \simeq P_a \cdot P_m \cdot \zeta_2 \cdot \zeta_3 \cdot \zeta_{ECAL} \quad (18)$$

where  $P_a$ ,  $\zeta_2$ ,  $\zeta_3$ , and  $\zeta_{ECAL}$  are, respectively, the probability for particle to pass through the entrance aperture, the inefficiencies of beam counters  $S_2$ ,  $S_3$  and ECAL counters to detect the particle.

To suppress this type of background the entrance aperture should be reduce to as much as possible size and should be closed by as high as possible efficiency counters  $S_{2,3}$ , as shown in Fig. 3, which act as the beam defining and also as the veto counters. Then, the background could be suppressed by requiring an absence of activity in the beam counters after detection of incoming muon. Assuming isotropic distribution of backscattered muons or decay positrons, inefficiency for particle detection in  $S_{2,3}$  of  $\simeq 10^{-2} - 10^{-3}$ , the diameter of the entrance aperture of  $\simeq 1$  cm, and inefficiency of the upstream ECAL detection  $\simeq 10^{-4}$  leads to the final suppression of this source of background down to the level of at least  $\simeq 10^{-13}$ .

- the leak of muonium atoms through the entrance aperture into the region of lower detection efficiency could also contribute be the disappearance rate of muonium. However, assuming that muoniums leaving the target are thermalized and have kinetic energy below eV (300 K), the effect is suppressed to a negligible level by closing the aperture with the counter  $S_3$ , as shown in Fig. 3.

In Table I contributions from the previously discussed background processes are summarized. The dominant background source is due to the absorption by passive materials of photons from the annihilation of slow positrons in the cavity. To cross-check this background, we estimate its level in the signal region by using available results from measurements of Ref.[3] and the proposal on the search for  $oPs \rightarrow \text{invisible}$  decay in vacuum of Ref.[19] in a different way. In Fig. 4 the expected distribution of energy deposition in the BGO calorimeter from the decays of  $8 \times 10^{12}$   $\mu^+$ 's stopped in the target is shown. The spectrum represents the sum of  $\mu^+ \rightarrow \text{all}$  and  $M \rightarrow \text{all}$  distributions. The part of the spectrum above  $\gtrsim 1$  MeV is calculated from the Michel spectrum convoluted with the ECAL (Gaussian) energy resolution. The peak around  $\simeq 1$  MeV is from the fraction of decay positrons ( $\simeq 10^{-4}$ ) with energy below of a few MeV that are stopped in the cavity, i.e. either in the target or in the cavity walls, and annihilate into 2 or 3 photons. The low energy tail below 1 MeV is described by a

TABLE I: Expected contributions to the total level of background from different background sources ( see text for details).

Source of background	Expected level
fake muon tag	$\lesssim 10^{-13}$
inefficiency of slow positrons detection <sup>a</sup>	$\lesssim 2 \times 10^{-12}$
$e^+ + A \rightarrow invisible$	$\lesssim 10^{-13}$
ECAL hermiticity	$\simeq 10^{-13}$
Total ( conservatively)	$\simeq 2.3 \times 10^{-12}$

<sup>a</sup> The threshold for energy deposited in the ECAL from the decay  $e^+$ 's annihilation is 100 keV.

function  $f(E_{e^+}) = f_1(E_{e^+}) + f_2(E_{e^+})$ , which is a sum of two distributions of the annihilation energy in the ECAL normalized to the same number of positrons annihilated in the cavity. The function  $f_1(E_{e^+})$  is an experimentally measured distribution taken from the experiment on  $Ps \rightarrow invisible$  [3] for positrons annihilated in the  $SiO_2$  target, which did not take into account the annihilation photon absorption in the cavity walls. The function  $f_2(E_{e^+})$  is taken from the proposal [19] and corresponds to the simulated energy deposition in the ECAL minus energy absorbed in the cavity walls. The sum function  $f(E_{e^+})$  is then extrapolated to zero energy resulting in prediction of about  $8 \pm 2$  background events in the signal region for  $8 \times 10^{12} \mu^+$ 's stop in the target, which is somewhat smaller, but still in a reasonable agreement with the conservative number of about 18 events obtained from Table 1. The error of the above estimate is defined by the uncertainty in the extrapolation procedure.

## B. Sensitivity of the proposed experiment

The significance of the  $M \rightarrow invisible$  decay discovery with such detector, scales as [72, 73]

$$S = 2 \cdot (\sqrt{n_s + n_b} - \sqrt{n_b}) \quad (19)$$

with

$$n_s = n_\mu \epsilon f Br(M \rightarrow invisible) t \quad (20)$$

and the branching ratio of the muonium invisible decay defined by

$$Br(M \rightarrow invisible) = \frac{n_s}{n_\mu \epsilon f t} \quad (21)$$

where and  $n_s$  is the number of observed signal events (or the upper limit of the observed number of events),  $n_b$  is the number of background events,  $n_\mu$  is the muon beam intensity,  $t$  is the experiment running time,  $\epsilon$  is the efficiency of the muonium production per incident muon, and factor  $f$  corresponds either to the total number of decayed  $M$  atoms ( $f \simeq 1$ ), or to the fraction of  $M$  atoms that decay presumably in vacuum, not in the target ( $f \simeq 0.033$ ).

Before defining the expected sensitivity, let us first discuss several additional limitation factors. The first one is related to the relatively long muon lifetime and the corresponding ECAL signal integration time. Indeed, to get the branching ratio  $Br(M \rightarrow invisible) \simeq 10^{-11}$ , the ECAL gate duration  $\tau_g$ , and hence the dead-time per trigger, has to be

$$\tau_g \gtrsim -\tau_\mu \times \ln(Br(M \rightarrow invisible)) \simeq 60 \mu s \quad (22)$$

in order to avoid background from the muon decays outside the gate. The best sensitivity is expected at integration gate  $\tau \simeq 60 \mu s$ , however further more complicated analysis compromising the level of this background and increase of the pile-up noise might be necessary. The pile-up energy, which corresponds to energy deposited in the BGO ECAL by an additional undetected and uncorrelated particle, increases values of the ECAL pedestals. The amount of additional energy in each BGO counter can be measured with the random trigger [3]. In the  $Ps$  experiment [3], for orthopositronium lifetime in the  $SiO_2$  aerogel target of 132 ns the ECAL gate duration  $\tau_{Ps}$  was chosen to be  $\simeq 2 \mu s$ . This resulted in distribution of the sum of pedestals of all ECAL counters corresponded to the efficiency of "zero" signal detection as a function of the energy threshold. In order to keep the energy threshold as low as possible an algorithm to sum up the energy of all the ECAL crystals can be employed by exploiting the granularity of the calorimeter and fixing a zero energy threshold for each individual crystal. Taking into account the ECAL granularity, the effective ECAL energy threshold can be significantly reduced from 80 keV, used to define the signal range for the  $o-Ps \rightarrow invisible$  decay [3], to about 20 keV having the overall signal efficiency above 95% [70]. In the proposed experiment the longer gate will lead to an increase of the pile-up and pick-up electronic noise and hence to the overall broadening of the signal range, approximately by a factor  $\sqrt{\tau_g/\tau_{Ps}} \simeq 5$  and, hence to an increase of the effective energy threshold roughly up to  $E_{th} \simeq 20 \text{ keV} \times 5 \simeq 100 \text{ keV}$ .

Another limitation factor is related to the dead time of Eq.(22) and, hence to the maximally allowed muon counting rate, which according to Eq.(22) has to be  $\lesssim 1/\tau_g \simeq 10^4 \mu^+/s$  to avoid significant pile-up effect. To minimize dead time, the trigger electronics has to reduce the rate of events accompanied by an energy deposition in the ECAL. For example, one could implement a fast first-level trigger rejecting events with the ECAL energy deposition greater than  $E_{th}$  and, hence run the experiment at the rate  $\simeq 1/\tau_\mu \simeq 5 \times 10^5 \mu/s$ . Assuming this rate, we anticipate  $8 \times 10^{12} \mu^+$  on target and production of about  $6 \times 10^{12}$  muonium atoms during 6 months of running time for the experiment. Out of them, about  $5.8 \times 10^{12} M$ 's decay in the target, while about  $2 \times 10^{11} M$ 's leave the target surface and decay in vacuum. For counting signal rate of  $\simeq 10^{-11}$  per incident muon, assuming beam intensity of  $\simeq 5 \times 10^5 \mu^+/s$  at  $\simeq 90\%$  efficiency, it would require 1 week to accumulate one signal event.

In the background free experiment one could expect a sensitivity in the  $M \rightarrow \text{invisible}$  decay branching ratio of the order of

$$Br(M \rightarrow \text{invisible}) \lesssim 10^{-12}, \quad (23)$$

assuming that in Eq.(21)  $n_s = 2.3$ . For  $M$ 's that decay in vacuum, the sensitivity is

$$Br^{\text{vac}}(M \rightarrow \text{invisible}) \lesssim 10^{-11}. \quad (24)$$

In the presence of background and in accordance with the SM prediction, the expected number of observed events in the signal region  $E \lesssim 100$  keV is

$$N_M \simeq 50 \pm 7 \text{ events} \quad (25)$$

out of which 18.4 events represent conservatively estimated overall background from Table 1. Taking into account (19), one can see that the observation of the  $M \rightarrow \text{invisible}$  decay with about  $5\sigma$  significance could be possible.

The statistical limit on the sensitivity of the proposed experiment to search for the decay  $M \rightarrow \text{invisible}$  due to transition into hidden sector is proportional to  $G_{MM'}^2$  and is set by its value, see (11). Thus, to improve the sensitivity of (24) larger amount of muonium atoms decaying in vacuum is required. Therefore, the improvement of the efficiency for thermal  $M$ 's production is crucial for further searches.

Note, that in the case of the signal observation, to cross check the result, one could replace the target with another one of the same density, but not capable of muonium producing, and run the experiment with suppressed  $M$  decays, see e.g. [74]. In this case the distribution of the energy deposition in the ECAL, shown in Fig.4 would contain mainly events from the decays  $\mu^+ \rightarrow \text{all}$  and the signal from the decays  $M \rightarrow \text{invisible}$  should disappear. In the case of observation of a higher than predicted  $M \rightarrow \text{invisible}$  decay rate, there is another important cross-check. Namely, as discussed in Sec. 3, one could slightly modify the experimental conditions without affecting the background, e.g. by increasing either the magnetic field in the cavity or the number of muonium collisions with residual gas molecules by increasing the gas pressure [19, 61]. These would suppress the muonium-mirror muonium oscillations, and the observed signal should vanish.

The performed analysis give an illustrative correct order of magnitude for the sensitivity of the proposed experiment. The simulations are performed without taking into account such effects as, e.g. pileup, and may be strengthened by more accurate and detailed Monte Carlo simulations of the concrete experimental setup.

## VI. CONCLUSION

Due to its specific properties, muonium is an important and interesting probe of the SM and physics be-

yond the SM both from the theoretical and experimental view points. In the SM the invisible decay of muonium atoms  $\mu^+ e^- \rightarrow \text{invisible}$  into two neutrinos is expected to be a very rare process with the branching fraction predicted to be  $Br(M \rightarrow \nu_\mu \nu_e) = 6.6 \times 10^{-12}$  with respect to the ordinary muon decay rate. This process has never been experimentally tested. Using the reported experimental results on searches for muonium-antimuonium conversion at PSI we set the first limit  $Br(M \rightarrow \text{invisible}) < 4.6 \times 10^{-3}$ , while still leaving a big gap of about nine orders of magnitude between this bound and the predictions.

To improve substantially the sensitivity, we proposed to perform an experiment dedicated to the search for the  $M \rightarrow \text{invisible}$  decay. The key point for the experiment is the presence of energy release from the annihilation of the low energy decay positrons in the detector. A feasibility study of the experimental setup show that the sensitivity of the search for this decay mode in branching fraction  $Br(M \rightarrow \text{invisible})$  at the level of  $10^{12}$  could be achieved. Thus, the SM prediction for the  $M \rightarrow \text{invisible}$  decay to exist at the level of  $Br(M \rightarrow \text{invisible}) \simeq 6.6 \times 10^{-12}$ , could be experimentally tested for the first time. We point out that the  $M \rightarrow \text{invisible}$  decay rate could be enhanced by non-SM contributions. For instance, in the framework of the mirror matter model if the coupling strength between  $M$  and  $M'$  is large enough, say  $G_{MM'} \gtrsim 10^{-4} G_F$ , the decay  $M \rightarrow \text{invisible}$  could occur at a rate as high as the SM one. If the proposed search results in a substantially higher branching fraction than the SM predictions, say  $Br(M \rightarrow \text{invisible}) \simeq 10^{-10}$ , this would unambiguously indicate the presence of new physics. A result in agreement with the SM prediction would provide a theoretically clean check of the pure leptonic bound state annihilation through charged current weak interactions, and provide constraints for further attempts beyond the SM.

The preliminary analysis shows that the quoted sensitivity could be obtained with a detector optimized for several its properties. Namely, i) the primary beam and the entrance aperture size, ii) the efficiency of the muonium production in the target and in vacuum, iii) the material composition and dimensions of the target and vacuum cavity, iv) the efficiency of the veto counters  $S_{1-4}$ , and v) the pile-up effect and zero-energy threshold in the ECAL are of importance.

We believe our proposal, when paired with an existing BGO calorimeter, provides interesting motivations for the experiment on search for the  $M \rightarrow \text{invisible}$  decay to be performed in near future. This low-energy experiment might be a sensitive probe of new physics that is complementary to collider experiments. For example, it could also significantly improve the recently obtained modest bounds on the  $\mu^+ \rightarrow \text{invisible}$  decay [18], pushing it down to the region  $Br(\mu^+ \rightarrow \text{invisible}) \simeq 10^{-12}$ . A bound in this region will be of interest for several extensions of the Standard Model, see e.g. [75]. The

required high numbers of muonium atoms can be presently produced at PSI [22], or could be available from high intensity muon beams at future facilities such as the PRISM source at J-PARC [76], the Project X at FNAL [77], or the neutrino factory [78].

## Acknowledgments

We thank P. Crivelli, D. Gorbunov, F. Guber, A. Ivashkin, A. Rubbia, V. Samoylenko and D. Sillou for discussions. The help of D. Sillou and A. Korneev in calculations is gratefully acknowledged. This work was supported by RFBR grant N 10-02-00468a.

---

[1] J. Beringer et al. (Particle Data Group), *Phys. Rev. D* **86**, 010001 (2012).

[2] S.N. Gninenko, N.V. Krasnikov, and A. Rubbia, *Phys. Rev. D* **67**, 075012 (2003).

[3] A. Badertscher, P. Crivelli, U. Gendotti, S.N. Gninenko, V. Postoev, A. Rubbia, V. Samoylenko and D. Sillou, *Phys. Rev. D* **75**, 032004 (2007).

[4] S.N. Ahmed et al., (SNO Collaboration), *Phys. Rev. Lett.* **92**, 102004 (2004).

[5] H.O. Back et al., (Borexino Collaboration), *Phys. Lett. B* **563**, 23 (2003).

[6] T. Araki et al., *Phys. Rev. Lett.* **96**, 101802 (2006).

[7] V.I. Tretyak, V.Yu. Denisov, Yu.G. Zdesenko, *JETP Lett.* **79**, 106 (2004), *Pisma Zh. Eksp. Teor. Fiz.* **79**, 136 (2004); *nucl-ex/0401022*.

[8] H.V. Klapdor-Kleingrothaus, I.V. Krivosheina, and I.V. Titkova, *Phys. Lett. B* **644**, 109 (2007).

[9] G.Banet et al., *Phys. Rev. Lett.* **99**, 161603 (2007).

[10] A.P. Serebrov et al., *Phys. Lett. B* **663**, 181 (2008).

[11] M. Sarrazin, G. Pignol, F.Petit, V.V. Nesvizhevsky, *Phys. Lett. B* **712**, 213 (2012).

[12] A. V. Artamonov et al. (E949 Collaboration), *Phys. Rev. D* **72**, 091102 (2005).

[13] M. Ablikim et al. (BES Collaboration), *Phys. Rev. Lett.* **97**, 202002 (2006).

[14] C.L. Hsu et al. (Belle Collaboration), *arXiv:1206.5948*.

[15] B. Aubert et al., (BABAR Collaboration), *Phys. Rev. Lett.* **103**, 251801 (2009).

[16] M. Ablikim et al. (BES Collaboration), *Phys. Rev. Lett.* **100**, 192001 (2008).

[17] P. Rubin et al., (CLEO Collaboration), *Phys. Rev. D* **75**, 031104 (2007).

[18] S.N. Gninenko, *Phys. Rev. D* **76**, 055004 (2007).

[19] P. Crivelli, A. Belov, U. Gendotti, S. Gninenko, A. Rubbia, *JINST* **5**, P08001 (2010); *arXiv:1005.4802 [hep-ex]*.

[20] W. Liu, M. G. Boshier, S. Dhawan, O. van Dyck, P. Egan, X. Fei, M. G. Perdekamp, V. Hughes, M. Janousch, K. Jungmann et al., *Phys. Rev. Lett.* **82**, 711 (1999).

[21] V. Meyer, S.N. Bagaev, P.E.G. Baird, P. Bakule, M.G. Boshier, A. Breitrock, S.L. Cornish, S. Dychkov, G.H. Eaton, A. Grossmann et al., *Phys. Rev. Lett.* **84** 1136 (2000).

[22] L. Willmann, P.V. Schmidt, H.P. Wirtz, R. Abela, V. Baranov, J. Bagaturia, W. H. Bertl, R. Engfer, A. Grossmann, V.W. Hughes et al., *Phys. Rev. Lett.* **82**, 49 (1999).

[23] V.W. Hughes, M. Grosse Perdekamp, D. Kawall, W. Liu (Yale U.), K. Jungmann, G. zu Putlitz, *Phys. Rev. Lett.* **87**, 111804 (2001).

[24] K. Kirch, *physics/0702143 [physics.atom-ph]*.

[25] V.W. Hughes and G. zu Putlitz, in: *Quantum Electrodynamics*, ed. T. Kinoshita, World Scientific, p. 822 (1990).

[26] K. Jungmann, in: *Muon Science*, eds. S.L. Lee, S.H. Kildey and R. Cywinsky, Inst. of Physics Publ., p. 405 (1999).

[27] K. Jungmann, *Nucl. Phys. B* **155**, 355 (2006).

[28] L. Willmann et al., *Phys. Rev. Lett.* **82**, 49 (1999).

[29] S.G. Karshenboim, *Phys. Rept.* **422**, 1 (2005).

[30] P.-J. Li, Z.-Q. Tan, and C.-E. Wu, *J. Phys. G* **14**, 525 (1988).

[31] B.Pontecorvo, *Zh.Exp.Theor.Fiz.* **33**, 549 (1958).

[32] G.Feinberg and S.Weinberg, *Phys.Rev.Lett.* **6**, 381 (1961).

[33] G.Feinberg and S.Weinberg, *Phys.Rev.* **123**, 1439 (1961).

[34] T.D. Lee, C.N. Yang, *Phys. Rev.* **104**, 256 (1956).

[35] I.Kobzarev, L.Okun, I.Pomeranchuk, *Sov. J. Nucl. Phys.*, **3**, 837 (1966).

[36] L.B. Okun, *Uspekhi Fiz. Nauk* **177**, 397 (2007); *hep-ph/0606202*.

[37] R. Foot, H. Lew, R. R. Volkas, *Phys. Lett. B* **272**, 67 (1991).

[38] Z.Berezhiani,R.Mohapatra, *Phys.Rev.D* **62**, 6607(1995); S E. Akhmedov, Z. Berezhiani and G. Senjanovic, *Phys. Rev. Lett.* **69**, 3013 (1992); Z. Berezhiani, A. Dolgov and R.N. Mohapatra, *Phys. Lett. B* **375**, 26 (1996); Z. Berezhiani, *Acta Phys. Pol. B* **27**, 1503 (1996).

[39] S.I.Blinnikov, *arXiv:0904.3609*; *astro-ph/9902305*; S.I.Blinnikov, M.Yu.Khlopov, *Sov.J.Nucl.Phys.* **36**, 472 (1982), *Yad.Fiz.* **36**, 809 (1982); *Sov. Astron.* **27**, 371 (1983), *Astron.Zh.* **60**, 632 (1983); M.Yu.Khlopov, *Cosmoparticle physics*, World Scientific, 1999; Z. Berezhiani, D. Comelli, F. L. Villante, *Phys. Lett. B* **503**, 362 (2001); Z. Berezhiani, P. Ciarcelluti, D. Comelli, F. L. Villante *Int. J. Mod. Phys. D* **14**, 107 (2005).

[40] Z. Berezhiani, *Int. J. Mod. Phys. A* **19**, 3775 (2004).

[41] P. Ciarcelluti, *Int. J. Mod. Phys. D* **14**, 187 (2005).

[42] Z.Berezhiani, S. Cassisi, P. Ciarcelluti and A. Pietrinferni, *Astropart. Phys.* **24**, 495 (2006).

[43] Z. Berezhiani, *Eur. Phys. J. ST* **163**, 271 (2008); *AIP Conf. Proc.* **878**, 195 (2006) [*hep-ph/0612371*].

[44] R. Foot, *Phys. Rev. D* **78**, 043529 (2008).

[45] R. Foot, *Phys. Rev. D* **80**, 091701 (2009).

[46] R. Foot, *Phys. Lett. B* **692**, 65 (2010).

[47] R. Foot, *arXiv:1203.2387*.

[48] L.Bento and Z.Berezhiani, *Phys. Rev. Lett.* **87**, 231304 (2001).

[49] B. Holdom, *Phys. Lett. B* **166**, 196 (1986).

[50] S.L. Glashow, *Phys. Lett.* **167**, 35 (1986).

[51] S.N. Gninenko, *Phys. Lett. B* **326**, 317 (1994).

[52] R. Foot and S.N. Gninenko, *Phys. Lett. B* **480**, 171 (2000).

[53] S.N.Gninenko, N.V.Krasnikov, V.A.Matveev and A.Rubbia, *Phys. Part. Nucl.* **37**, 321 (2006).

[54] T. Mitsui, R. Fujimoto, Y. Ishisaki, Y. Ueda, Y. Yamazaki, S. Asai and S. Orito, *Phys. Rev. Lett.* **70**, 2265 (1993).

[55] S.N. Gninenco, *Int. J. Mod. Phys. A* **19**, 3833 (2004).

[56] Z. Berezhiani and L. Bento, *Phys. Lett. B* **635**, 253 (2006).

[57] Z. Berezhiani and F. Nesti, *Eur. Phys. J. C* **72**, 1974 (2012); arXiv:1203.1035 [hep-ph].

[58] A.Y. Ignatiev and R.R. Volkas, *Phys. Lett. B* **487** 294 (2000)294.

[59] Wen-sheng Li, Peng-fei Yin, and Shou-hua Zhu, *Phys. Rev. D* **76**, 095012 (2007).

[60] Jian-Wei Cui, Hong-Jian He, Lan-Chun Lu, Fu-Rong Yin, *Phys. Rev. D* **85**, 096003 (2012).

[61] S.V. Demidov, D.S. Gorbunov, A.A. Tokareva, *Phys. Rev. D* **85**, 015022 (2012).

[62] L. Willmann and K. Jungmann, *Lect. Notes Phys.* **499**, 43 (1997); hep-ex/9805013.

[63] D.B. Chitwood et al. (MuLan Collaboration), *Phys. Rev. Lett.* **99**, 032001 (2007); arXiv:0704.1981.

[64] R. Abela, F. Foroughi and D. Renker, *Z. Phys. C* **56**, S240 (1992).

[65] K. Woodle et al., *Z. Phys. D* **9**, 59 (1988); see also A. C. Janissen et al., *Phys. Rev. A* **42**, 161 (1990); G. A. Beer et al., *Phys. Rev. Lett.* **57**, 671 (1986); R. F. Kiefl et al., *Phys. Rev. B* **26**, 2432 (1982); G. M. Marshall et al., *Phys. Lett.* **65 A**, 351 (1978).

[66] G.M. Marshall et al., *Phys. Lett. A* **65** , 351 (1978).

[67] A. Antognini, P. Crivelli, T. Prokscha, K. S. Khaw, B. Barbiellini, L. Liszkay, K. Kirch1, K. Kwuida, E. Morenzoni, F. M. Piegsa, Z. Salman, and A. Suter, *Phys. Rev. Lett.* **108**, 143401 (2012).

[68] S. Agostinelli et al. (GEANT4 Collaboration), *Nucl. Instrum. Meth. A* **506**, 250 (2003); J. Allison et al. (GEANT4 Collaboration) *IEEE Trans. Nucl. Sc.* **53**, 270 (2006).

[69] G. Czapek at el., *Phys. Rev. Lett.* **70**, 17 (1993).

[70] P. Crivelli, Ph.D. thesis, No. 16617, ETH Zürich, Switzerland (2006).

[71] D. B. Cassidy, A. W. Hunt, P. Asoka-Kumar, B. V. Bhat, T. E. Cowan, R. H. Howell, K. G. Lynn, A. P. Mills, Jr., J. C. Palathingal, and J. A. Golovchenko, *Phys. Rev. C* **64**, 054603 (2001).

[72] S.I. Bityukov and N.V. Krasnikov, *Mod. Phys. Lett A* **13**, 3235 (1998); hep-ph/0204326.

[73] S.I. Bityukov and N.V. Krasnikov, *Nucl. Instr. Meth. A* **534**, 152 (2004).

[74] G.S. Atoyan, S.N. Gninenco, V.I. Razin and Yu.V. Ryabov, *Phys. Lett. B* **220**, 317 (1989).

[75] S.L. Dubovsky, V.A. Rubakov, P.G. Tinyakov, *JHEP* **0008**, 041 (2000).

[76] A. Sato, *Nucl. Phys. A* **721**, 1083 (2003).

[77] J.L. Hewett et al., arXiv:1205.2671 [hep-ex].

[78] J. Aysto et al., hep-ph/0109217.